Journal of Electroanalytical Chemistry 850 (2019) 113433

Contents lists available at ScienceDirect

Journal of Electroanalytical Chemistry

journal homepage: www.elsevier.com/locate/jelechem

Short communication

Effect of deposition parameters on spray pyrolysis synthesized CuO nanoparticle thin films for higher supercapacitor performance

S.K. Shinde [a], S.M. Mohite [b], A.A. Kadam [c], H.M. Yadav [d], G.S. Ghodake [a], K.Y. Rajpure [b,*], D.S. Lee [e], D.-Y. Kim [a,*]

[a] Department of Biological and Environmental Science, College of Life Science and Biotechnology, Dongguk University, 32 Dongguk-ro, Biomedical Campus, Ilsandong-gu, Siksa-dong, 10326 Goyang-si, Republic of Korea
[b] Electrochemical Materials Laboratory, Department of Physics, Shivaji University, Kolhapur 416004, India
[c] Research Institute of Biotechnology and Medical Converged Science, Dongguk University, Biomedi Campus, Ilsandong-gu, Goyang-si, Gyeonggi-do 10326, Republic of Korea
[d] Department of Energy and Materials Engineering, Dongguk University, Seoul 04620, Republic of Korea
[e] Department of Environmental Engineering, Kyungpook National University, 80 Daehak-ro, Buk-gu, Daegu 41566, Republic of Korea

ARTICLE INFO

Article history:
Received 14 March 2019
Received in revised form 28 July 2019
Accepted 27 August 2019
Available online 28 August 2019

Keywords:
Spray pyrolysis
CuO thin film
Nanoparticles
Supercapacitor

ABSTRACT

In this study, copper oxide (CuO) thin films were synthesized at different deposition temperatures on fluorine doped tin oxide coated glass (FTO) substrates by spray pyrolysis for supercapacitor applications. The physical and electrochemical properties of the as-synthesized CuO samples were characterized via different analytical techniques such as X-ray diffraction (XRD), X-ray photoelectron spectroscopy, scanning electron (SEM) microscopy, surface wettability tests, and electrochemical measurements. The results showed that the deposition temperature affected their structural, morphological, and supercapacitor properties. The higher specific capacitance and extensive charge/discharge capability of the nanoparticle-like CuO thin films demonstrated their suitability as outstanding candidates in electrochemical applications. The evaluated specific capacitance further confirmed the effect of the deposition temperature on the supercapacitor performance of the CuO electrodes; its values for the thin films synthesized at 300, 350, and 400 °C were 363, 691, and 487 F g^{-1}, respectively, at a scan rate of 5 mV s^{-1} in a 2 M Na_2SO_4 aqueous electrolyte. Hence, this study demonstrates that the surface morphology and electrochemical supercapacitive properties of materials are dependent on the deposition temperature of CuO thin films.

1. Introduction

The world is currently demanding for new energy storage/conversion devices that are lightweight, eco-friendly, and inexpensive. Various types of such devices including capacitors [1], batteries [2], fuel cells [3,4], solar cells [5], and supercapacitors are available commercially [6–8]; among them, supercapacitors are better than capacitors and batteries because of properties such as their high energy and power densities [7-10], fast charging/discharging, and long-term cycling stability [11,12]. These properties are useful in various applications, including in portable media players, digital electronics and cameras, medical devices, railways, street lights, and power banks [9–13]. Supercapacitors can be classified as EDLCs and pseudocapacitors based on their charge storage mechanism [7, 10–15]. This mechanism is related to non-faradaic capacitance resulting from the ion transformation in the Helmholtz double layer between the electrode and electrolyte in the former [11,13–19] and to faradaic reactions involving electrostatic charge storage in the latter [20,21].

Researchers have been investigating various metal oxide materials such as ruthenium oxide, iron oxide, manganese dioxide, nickel oxide, and copper oxide as well as conducting polymers for use in supercapacitors [8–13,20,21]. Among them, ruthenium oxide has exhibited high specific capacitive, high power density, and good stability, but its commercial distribution is hindered by its higher cost and environmental impact compared to those of other binary metal oxides. Dubal et al. [22] synthesized CuO via chemical bath deposition (CBD), reporting three different nanostructures that affected the supercapacitor performance; they attained a higher specific capacitance of 346 F g^{-1} with microwoolen-like CuO nanosheets at a scan rate of 5 mV s^{-1}. Sagu et al. [23] deposited CuO thin films as photoactive materials on FTO-coated glass substrates using electrodeposition, and measured a highest photocurrent density of 2.1 mA cm^{-2} in a 1 M NaOH electrolyte. Shu et al. [24] fabricated CuO thin films on a Cu foam by electrochemical anodization; they observed single-phase copper oxide with good electrochemical properties and a specific capacitance of around 600 mF cm^{-2} in a 2 M KOH aqueous electrolyte at a current density of 1 mA cm^{-2} and excellent cycling stability with around 94% retention

* Corresponding authors.
E-mail addresses: rajpure@yahoo.com (K.Y. Rajpure), sbpkim@dongguk.edu (D.-Y. Kim).

https://doi.org/10.1016/j.jelechem.2019.113433
1572-6657/

after 10,000 cycles. Shinde et al. [25] prepared CuO thin films on copper foils via the SILAR method for supercapacitor and biocompatibility applications; they reported that the e-beam irradiation affected the performance of the CuO electrodes and that the 20 kGy-irradiated samples exhibited the maximum specific capacitance in 1 M KOH.

Many researchers are currently testing CuO-based nanomaterials for electrochemical applications because CuO is cheap, leads to low environmental impact, and provides good electrochemical stability and easy fabrication [26,27]. In addition to the above mentioned SILAR, physical and chemical CuO deposition techniques include electrodeposition methods [28,29], spin coating [30], thermal oxidation [31], chemical bath deposition [32], hydrothermal deposition [33], sol–gel processing [34], surface oxidation [35], jet nebulizer spray pyrolysis (JNSP) [36], electrodeposition [37], the solution method [38], microwave irradiation [39], chemical precipitation [40], and solid-state chemical reactions [41]. Among them, the spray pyrolysis technique (SPT) is quite attractive for the fabrication of electrodes for different applications such as in supercapacitors, solar cells, and gas sensors because of the associated low deposition time, cost, and material loss; ease of electrode preparation; and large area deposition.

In this report, novel CuO thin films were synthesized using the cost-effective SPT to obtain uniform and well-adherent films. The effect of the deposition temperature on the structure, surface morphology, wettability, and electrochemical properties were investigated in detail. In addition, the electrochemical supercapacitive properties of the fabricated CuO thin films were tested using various electrolytes.

2. Experimental

2.1. Materials

Copper (II) chloride dihydrate (99.0%) and KOH pellets were purchased from S. D. Fine-Chem Ltd. (India) and Thomas Baker (Chemicals) Pvt. Ltd. (India), respectively. All chemicals were used without further purification. The FTO-coated glass substrates were prepared using a homemade SPT system (transparency = 85%, sheet resistance = 10 $\Omega\ cm^{-2}$).

2.2. Preparation of CuO thin films

Polycrystalline CuO films were synthesized via SPT [42]. Cupric chloride (0.4262 g) was dissolved in double-distilled water (50 mL) to obtain the precursor solution that was successively sprayed onto the preheated bare and FTO-coated glass substrate at various deposition temperatures ranging between 300 and 450 °C at intervals of 50 °C. Parameters such as the amount of solution (50 mL), solution concentration (50 mM), and spray rate (3 mL min^{-1}) were kept constant during the spray deposition.

2.3. Characterization of CuO thin films

The phase and polycrystalline nature of the synthesized CuO films were examined via X-ray diffractometry using a Bruker D2 PHASER table-top powder diffractometer with Cu K_α radiation (wavelength = 1.5406 Å). The surface morphology was characterized by a JEOL JSM-6360 microscope [43,44].

2.4. Electrochemical measurements

The electrochemical performance of the produced CuO thin films was evaluated through cyclic voltammetry (CV), galvanostatic charge/discharge tests, and electrochemical impedance (EIS) measurements using a CHI-660-D workstation. A reference electrode probe and a counter electrode probe were connected to an Ag/AgCl electrode and a thin platinum foil, respectively. A working electrode probe was connected to the CuO/FTO-coated electrode and immersed in a 2 M Na_2SO_4 electrolyte. EIS measurements were performed between 1 Hz and 100 kHz with an alternating current (AC) amplitude of 10 mV and a bias potential of 0.4 V.

3. Results and discussions

3.1. Structural study

The phase and crystalline nature of the as-synthesized samples were determined by XRD. Fig. 1 (a–d) shows the XRD patterns of the CuO thin films synthesized at different deposition temperatures of 300, 350, 400, and 450 °C, respectively. The two most intense peaks observed at 35.47° and 38.52°, corresponding to the planes (002) and (11-1), indicated a monoclinic phase with cubic crystal structure for all of the samples [20]; all the peaks could be well matched with those of the Joint Committee on Powder Diffraction Standard (JCPDS) card number 05-0661 [26]. No other impurity peaks owing to CuO and $Cu(OH)_2$ were observed [11]. The results revealed parallel XRD patterns for all the samples with changes only in the peak intensities, whose decrease above 400 °C was probably due to the decomposition of the CuO solution at such high temperatures. In addition, an increase in the peak intensities with increasing the deposition temperature from 300 to 350 °C was noticed, while a further increase in the deposition temperature decreased the peak intensity and broadened the peaks, suggesting a reduced particle size. Similar trends were observed for the results obtained from the surface morphology of the samples [45], as described in Section 3.3. The crystallite (D) values of CuO thin films synthesized at different deposition temperatures was calculated by using Scherrer's formula for plane (11-1):

$$D = \frac{0.9\lambda}{\beta \cos\theta} \quad (1)$$

where D is the crystallite size and β is the full width at half of its maximum intensity. The calculated values of the crystallite sizes were 87, 61, 23, and 43 nm for CuO thin films deposited at 300, 350, 400, and 450 °C, respectively. The decreasing crystallite size must be due to the decomposition of CuO ions at a higher deposition temperature.

3.2. X-ray photoelectron spectroscopy (XPS) study

XPS analysis was performed to advance examine the chemical state, valence state of the elements, and chemical composition of the CuO samples prepared at an optimized deposition temperature of 350 °C.

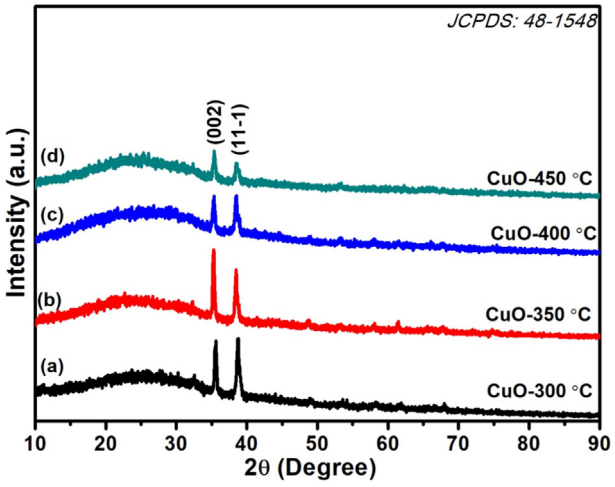

Fig. 1. XRD patterns of CuO thin films deposited at (a) 300, (b) 350, (c) 400 and (d) 450 °C deposition temperatures by spray pyrolysis method.

Fig. 2a displays the survey spectrum of the CuO thin films deposited by spray pyrolysis, which confirms the presence of both copper and oxygen and the formation of pure copper oxides without any impurity. Fig. 2 (b–d) shows the core level spectrum of the constituent copper (Cu 2p), oxygen (O 1s), and carbon (C), respectively. Peaks were detected at 932.91 and 530.19 eV, which respectively correspond to the binding energies of copper and oxygen and therefore confirm CuO formation in the samples. The most intense peaks, at 932.91 and 953.60 eV, matched the binding energies of Cu $2p_{3/2}$ and Cu $2p_{1/2}$, respectively, as shown in Fig. 2(b) [46]. Furthermore, one more satellite peak can be observed at 940.84 eV, respectively, and completing assignment of the Cu 2p level [47]. Fig. 2(c) shows the core level spectrum of O 1s; the peak at 530.19 eV suggests the presence of oxygen in the synthesized CuO thin films [45]. A peak at 284.60 eV corresponding to carbon was also observed (Fig. 2d). Thus, the XPS analysis was in good agreement with the XRD results.

3.3. Surface morphology study

The surface morphology of the as-prepared CuO films was studied by SEM. Fig. 3 (a–f) shows the SEM images of the CuO nanostructures prepared at different deposition temperatures of 300, 350, and 400 °C under different magnifications. All the CuO thin films were fully covered with uniform and homogeneous distributions of nanoparticle-like nanostructures on the FTO-coated glass substrate [11]. Fig. 3 (a, b) shows the SEM images of CuO thin films prepared at 300 °C deposition temperature by spray pyrolysis. The substrate was covered with hexagonal nanorod-like nanostructures. At a higher magnification, we observed that the surface of CuO films was not fully covered since the deposition temperature was insufficient for complete decomposition of CuO. To resolve this issue, we increased the deposition temperature to 350 °C, at which the CuO thin films showed compact and uniform growth of nanoparticle-like nanostructures over the substrate: this suggested that a deposition temperature of 350 °C is suitable for the decomposition of CuO (Fig. 3 (c, d))[48]. XRD analysis strongly supported these conclusions drawn on the surface morphology of the CuO thin films (Fig. 1). These particles were much smaller (~80–100 nm) than those observed in the case of the other two CuO thin films, indicating that it provided a greater reactive surface area during the supercapacitor performance testing [49]. On increasing the deposition temperature from 350 to 400 °C (Fig. 3(e, f)), the CuO films became uniformly covered with an interconnected nanoparticle-like network. At a higher magnification, it can be clearly seen that the size of nanoparticles (~150–200 nm) increased slightly compared to that of the other CuO thin films. Finally, based on the SEM results, we concluded that the CuO deposited at 350 °C exhibited the uniform distribution of particles as well as more compact and uniform particle sizes (~80–100 nm). This led to better results than what was achieved by the other two samples. Since the smaller particles provided a greater reactive surface area, fast reaction between CuO and electrolyte, and fast charging/discharging [48, 49].

3.4. Wettability study

Characterizing the surface wettability is very useful to identify the relationship between liquid electrolytes and working electrodes: a high wettability indicates a low contact angle between the working electrode and vice versa [50]. In this study, we performed contact angle measurements to decide the effect of the deposition temperature on the CuO thin films and their quality in terms of supercapacitor applications. The results, shown in Fig. 4, confirmed the influence of the temperature on the surface wettability of the films, since the calculated contact angle increased from 64° to 76° on increasing the deposition temperature from 300 to 350 °C. However, on further increase of the deposition temperature to 400 °C, the contact angle increased again from 76° to 87°, which may be due to significant changes occurring in the

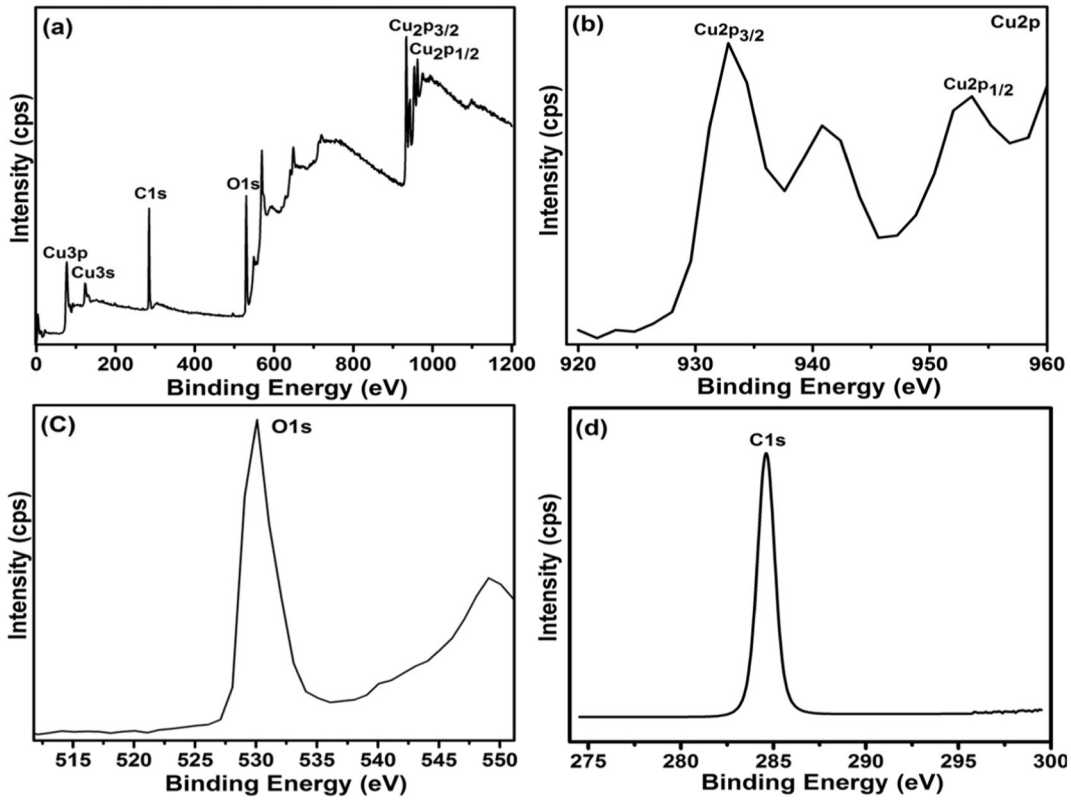

Fig. 2. (a) Survey spectrum, (b) high-resolution spectrum of Cu 2p level, (c) high-resolution spectrum of O1s level, and (d) high-resolution spectrum of C1s level for the thin film deposited at 350 °C temperature by spray pyrolysis.

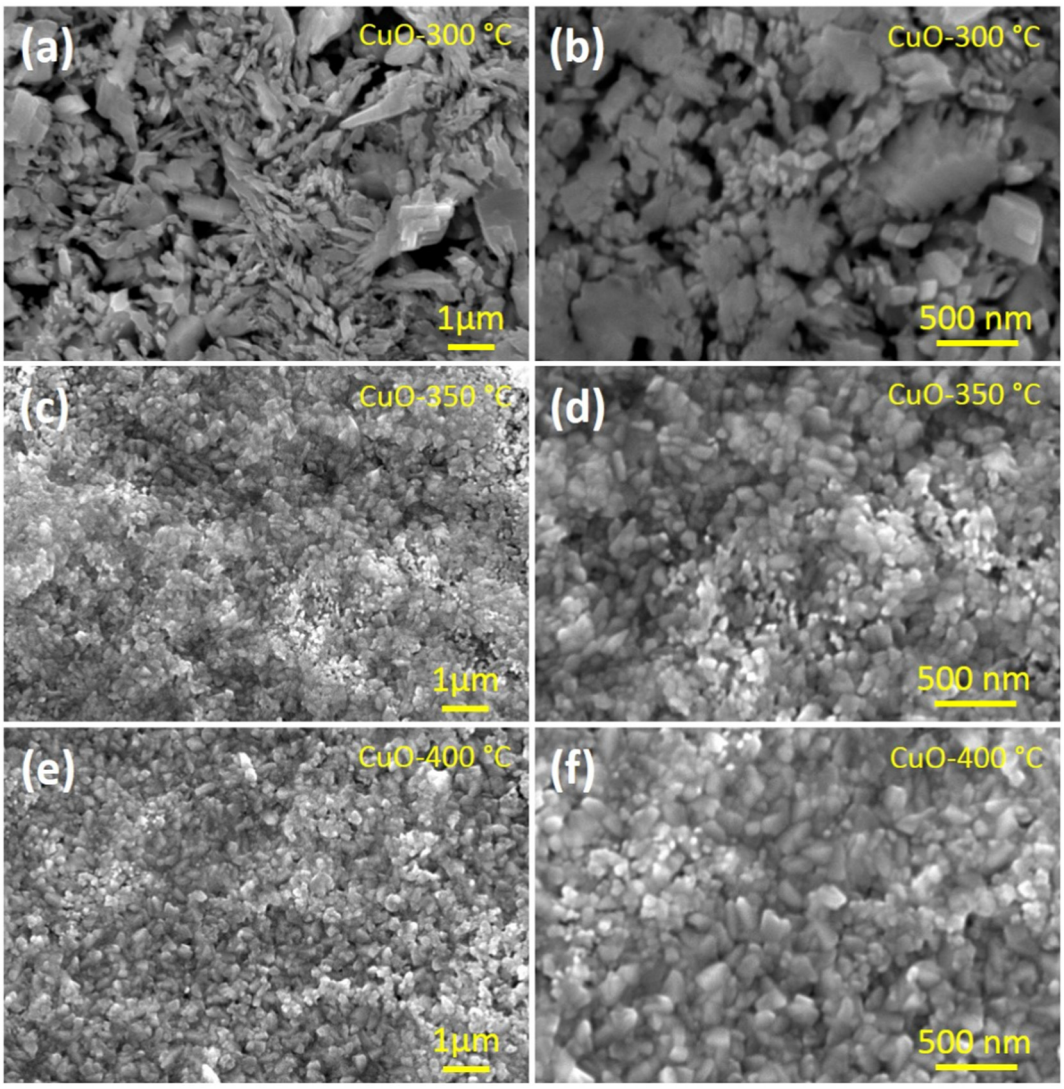

Fig. 3. SEM images of CuO thin films deposited at (a, b) 300 °C, (c, d) 350 °C, and (e, f) 400 °C deposition temperatures with different magnifications.

nanoparticles size, as demonstrated by SEM investigation. The increase in the contact angle was thus related to the decomposition of CuO particles at a higher deposition temperature. These results suggest a hydrophilic nature of the surface of the as-prepared CuO films, which is very beneficial in ion transformation during contact between an aqueous electrolyte and CuO functioning as the working electrode. Hence, based on the surface wettability results, the synthesized CuO samples can be considered suitable for offering appropriate electrolyte/electrode interface and electrochemical results [50].

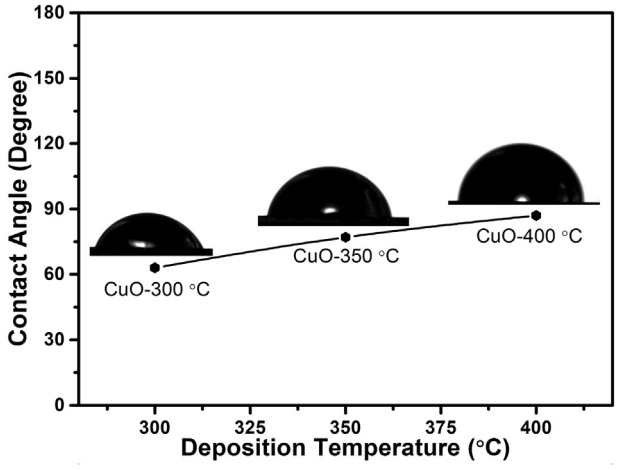

Fig. 4. Surface wettability of CuO thin films deposited at different deposition temperatures from 300, 350 and 400 °C, respectively.

3.5. Electrochemical supercapacitive properties

The supercapacitive properties of the spray-deposited CuO electrodes were studied by CV and galvanostatic charge/discharge (GCD) analysis using a three-electrode system in a 2 M Na_2SO_4 electrolyte. Fig. 5(a–c) shows the CV curves of the CuO electrodes prepared at different deposition temperatures of 300, 350, and 400 °C, respectively, which obtained at scan rates of 5–100 mV s^{-1} in the potential window of 0.0–0.45 V. The voltammograms revealed a similar nature for all samples, with the only difference noted in the current density, which was 18.9, 44.2, and 29.5 mA·cm^{-2} for the samples deposited at 300, 350, and 400 °C, respectively. These results suggest that the electrode prepared at 350 °C was much larger than the other two, and therefore showed a significant increase in the specific capacitance [50–52]. Strong anodic and cathodic peaks were observed at 0.35 and 0.45 V, respectively, which may be due to the faradaic redox reactions between Cu (I) and Cu (II) [51–53]. All voltammograms clearly indicate that the

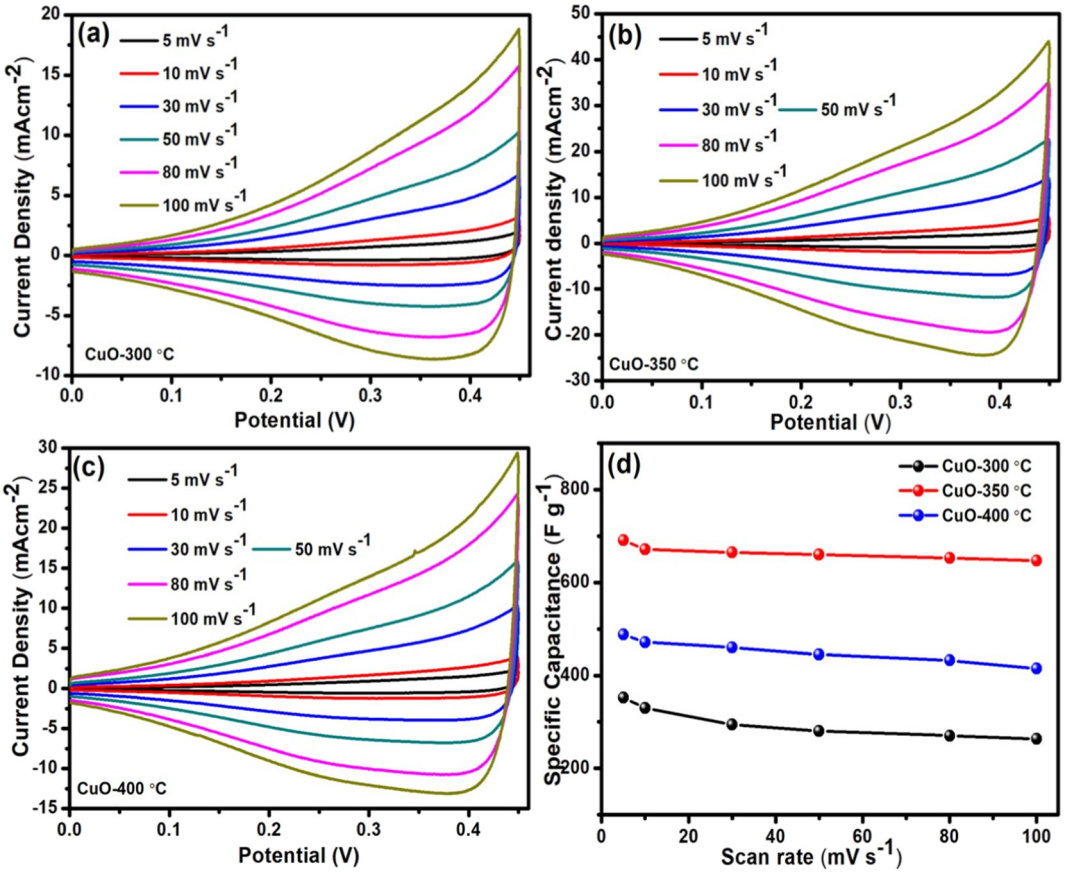

Fig. 5. (a–c) Cyclic voltammetry (CV) curves of CuO thin films deposited at 300, 350, and 400 °C at various scan rates of 5–100 mV s^{-1} in 2 M Na_2SO_4, respectively. (d) Variation in specific capacitance with the scan rate for CuO thin films deposited at various temperatures.

CuO samples were pseudocapacitor-type electrode materials [53–55]. Fig. 5(d) shows the specific capacitance of the CuO electrodes deposited at different temperatures investigated under various scan rates of 5–100 mV s^{-1} in a 2 M Na_2SO_4 aqueous electrolyte. The maximum specific capacitance obtained was for the CuO electrodes deposited at 350 °C, because of the smaller nanoparticle size and greater active surface area involved compared to those of the other electrodes. The values of specific capacitance were 363, 691, and 487 F g^{-1} for the samples deposited at 300, 350, and 400 °C, respectively, at 5 mV s^{-1} in a 2 M Na_2SO_4 electrolyte. The CuO samples showed higher specific capacitance than those previously reported, shown by a comparison in Table 1. Based on the CV results, we concluded that the material we investigated is useful for ion exchange processes as it exhibits high rate stability and superior mass transport.

To understand the supercapacitive properties of the synthesized CuO electrodes in further detail, we performed GCD testing at different current densities in a 2 M Na_2SO_4 electrolytes. Fig. 6 (a–c) shows the GCD test results for the CuO electrodes at different current densities between 0.5 and 6 mA cm^{-2} in a 2 M Na_2SO_4 electrolyte that had been synthesized at different deposition temperatures of 300, 350, and 400 °C, respectively. The specific capacitance was calculated using the following equation [53].

$$C = \frac{I_d \times \Delta t}{m \times \Delta V}$$

where C, I_d, Δt, m and ΔV are the specific capacitance, discharge current, discharge time, potential and mass of the CuO electrodes, respectively. At a current density of 0.5 mA cm^{-2}, the calculated C values were 247, 496, and 306 F g^{-1} for the CuO electrodes deposited at temperatures 300, 350, and 400 °C, respectively (Fig. 6(d)), demonstrating the superiority of the CuO electrodes prepared at 350 °C, likely owing to its porous

Table 1
Comparison study of electrochemical performance of CuO thin films.

Method	Specific capacitance (F g^{-1})	Electrolytes	Scan rates (mV s^{-1})/current density (mA cm^{-2})	References
Chemical bath deposition	411 F g^{-1}	1 M Na_2SO_4	5 mV s^{-1}	[16]
In situ oxidation reaction	594.27 F g^{-1}	6 M KOH	2 mA cm^{-2}	[17]
Polyol reduction method	173.2 F g^{-1}	2 M KOH	5 mV s^{-1}	[19]
Solvothermal calcination	677 F g^{-1}	3 M KOH	1 A g^{-1}	[20]
In situ method	600 mF cm^{-2}	2 M KOH	1 mA cm^{-2}	[24]
SILAR	511 F g^{-1}	1 M KOH	10 mV s^{-1}	[25]
Hydrothermal method	80 F g^{-1}	1 M Na_2SO_4	10 mV s^{-1}	[33]
Electrodeposition	601 F g^{-1}	6 M KOH	2 A g^{-1}	[37]
Solid-state chemical reaction	308 F g^{-1}	1 M KCl	4 mA cm^{-2}	[41]
Template-free growth	569 F g^{-1}	6 mM KOH	5 mA cm^{-2}	[53]
Solution combustion	185 F g^{-1}	1 M Na_2SO_4	5 mV s^{-1}	[58]
Spray pyrolysis	691 F g^{-1}	2 M Na_2SO_4	5 mV s^{-1}	Current study

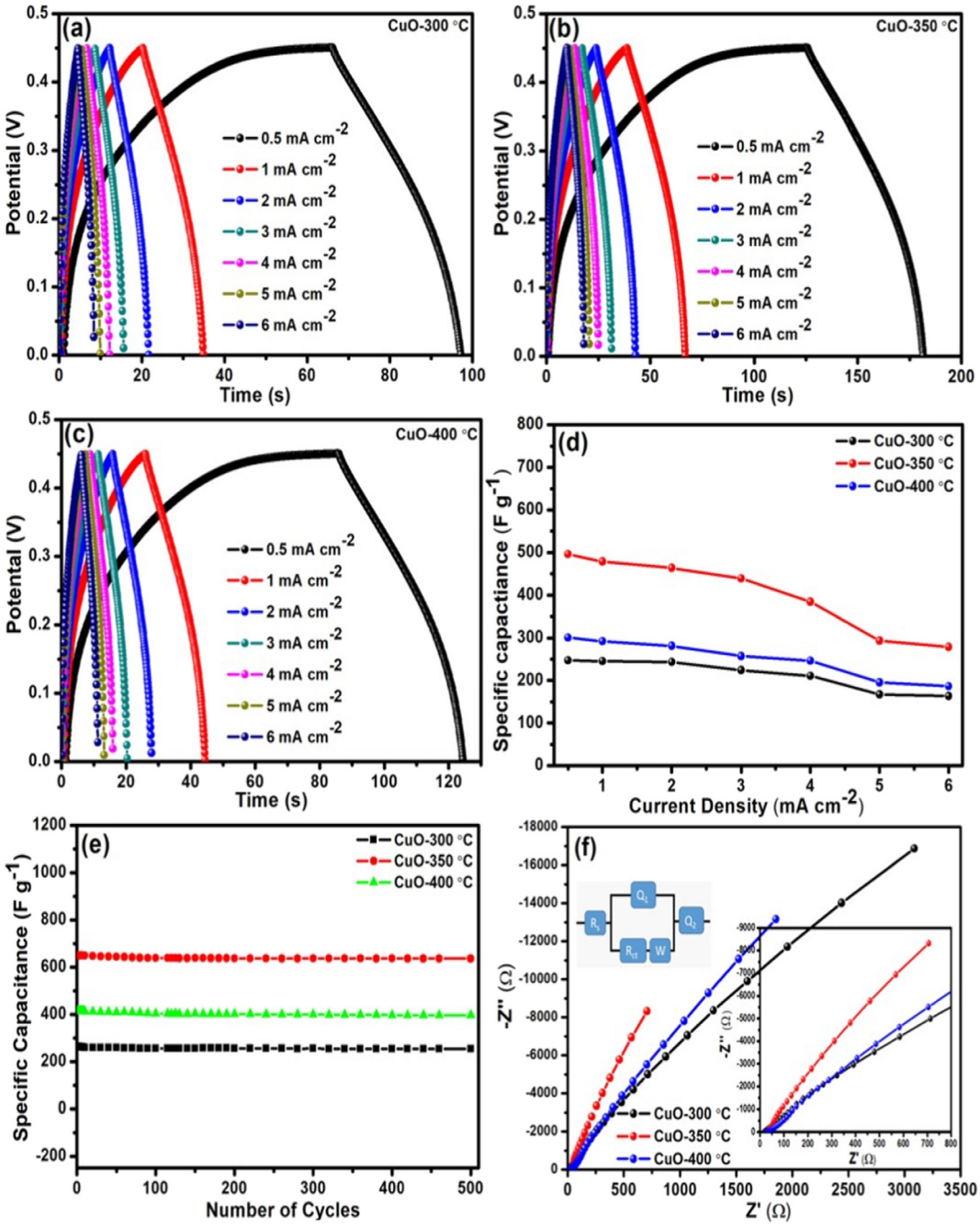

Fig. 6. (a–c) Galvanostatic charge/discharge curves of CuO thin films deposited at 300, 350, and 400 °C deposition temperatures with various current densities from 0.5 to 6 mA cm^{-2}, in potential window 0 to 0.45 V, respectively, (d) variation of specific capacitance with respect to current densities from 0.5 to 6 mA cm^{-2} of CuO films deposited at various deposition temperatures, (e) cycling stability of CuO thin films with respect to number cycles at 100 mV s^{-1} scan rate, (f) Nyquist plots of CuO films deposited at various deposition temperatures from 300 to 400 °C by spray pyrolysis method, and inset shows the equivalent circuit.

nanostructure; in particular, the higher specific capacitance of the CuO thin films may be attributed to the nanoparticle size that provided a larger active surface and greater stability during the electrochemical reaction [51–53]. The specific capacitance decreased with increasing current density, perhaps owing to the absence of the Faradic redox reaction as well as because of the size of nanostructures and porosity and resistance of the CuO electrode: the current densities for the electrode prepared as 350 °C were 496, 478, 463, 438, 384, 293, and 278 F g^{-1} under currents of 0.5, 1, 2, 3, 4, 5, and 6 mA cm^{-2}, respectively. The *C* values were higher than those previously reported [28–33,56,57]. For example, Gholivand et al. [58] achieved a specific capacitance of 76 F g^{-1} at 100 mV s^{-1} in a 2 M Na_2SO_4 electrolyte and Dubal et al. [59], who fabricated CuO electrodes using CBD for supercapacitor applications, observed cauliflower-like structures exhibiting a current density of 2 mA cm^{-2} for a specific capacitance of 162 F g^{-1}. To confirm the long-term cycling stability of the as-synthesized CuO thin films, we performed cycling tests for 1000 cycles at 100 mV s^{-1} in a 2 M Na_2SO_4 electrolyte. Fig. 6e shows the specific capacitance of the CuO thin films prepared at different deposition temperatures with the respective number of cycles at a scan rate of 100 mV s^{-1}. Fig. 6e clearly shows that the specific capacitance decreased in the first 200 cycles, beyond which it remained almost constant for up to 1000 cycles, indicating that these CuO electrodes show good long-term electrochemical stability. These results could be due to the surface morphology and the low resistance and stability of the CuO thin films deposited by the spray pyrolysis method.

Table 2
EIS parameters of CuO thin films prepared at different deposition temperatures.

Parameters/thin films	CuO-300 °C	CuO-350 °C	CuO-400 °C
R_S	30	6.94	27.45
R_{ct}	1.763E5	4.703E4	5.178E6
W	6.459E−8	4.661E−6	1.548E−5

3.6. EIS measurements

To gain further details on the electrical conductivity of the as-synthesized CuO electrodes, we performed EIS measurements. Fig. 6f shows the Nyquist plots and the inset shows the corresponding equivalent circuit. The supercapacitor-like nature of the CuO thin films can be seen in Fig. 6f. The solution resistance (R_s), charge transfer resistance (R_{ct}), and Warburg (W) impedance was estimated to understand the relationship between the Na_2SO_4 electrolyte and the as-synthesized CuO electrodes. As depicted in Table 2, no significant difference was noted in terms of R_{ct} among these three CuO samples, while their R_s values differed significantly [60], which may be due to the porous nanoparticle-like nanostructures that provided a larger surface area during the electrochemical testing. The R_s values were 30, 6.94, and 27.45 Ω for samples deposited at 300, 350, and 400 °C, respectively. Hence, the electrode prepared at 350 °C exhibited the lowest R_s value, indicating its superiority in ion exchange/ion transformation at the electrode/electrolyte interface [61–63].

4. Conclusions

We conducted a comparative study of CuO-based electrodes fabricated at different deposition temperatures via spray pyrolysis, which is an easy, low-cost, and eco-friendly technique, on FTO-coated glass substrates for supercapacitor applications. The effects of the spray deposition temperature on the supercapacitor performance were studied in detail based on cyclic voltammetry, specific capacity, charge/discharge, and EIS measurements. The sample deposited at 350 °C exhibited outstanding electrochemical performance, which was better than that shown by the samples prepared at 300 and 400 °C: it exhibited an excellent specific capacitance of 691 F g^{-1} at 5 mV^{-1}. The significant improvement observed in the supercapacitor properties was attributed to the nanoparticle size and polycrystalline structure of the CuO thin films, which provided easy ion transport and electron exchange during the reaction. The obtained results demonstrate that CuO thin films can be suitable candidates as electrode materials for supercapacitor applications.

Acknowledgments

This work was supported by the Dongguk University Research Fund of 2018–2020.

References

[1] P. Simon, Y. Gogotsi, B. Dunn, Where do batteries end and supercapacitors begin? Science 343 (2014) 1210–1211.
[2] Z. Yu, M. McInnis, J. Calderon, S. Seal, L. Zhai, J. Thomas, Functionalized graphene aerogel composites for high-performance asymmetric supercapacitors, Nano Energy 11 (2015) 611–620.
[3] S. Samanta, A.K. Nayak, A. Mukherji, D. Pradhan, B. Satpati, R. Srivastava, Flower-shaped self-assembled $Ni_{0.5}Cu_{0.5}Co_2O_4$ porous architecture: a ternary metal oxide as a high-performance charge storage electrode material, ACS Applied Nano Materials 1 (2018) 5812–5822.
[4] D. Zhou, Z.D. Deng, Ultra-low-head hydroelectric technology: a review, Renew. Sust. Energ. Rev. 78 (2017) 23–30.
[5] K.T. Sanders, Critical review: uncharted waters? The future of the electricity-water nexus, Environ. Sci. Technol. 49 (2015) 51–66.
[6] M.V. Reddy, G.V. Subba Rao, B.V.R. Chowdari, Metal oxides and oxysalts as anode materials for Li ion batteries, Chem. Rev. 113 (2013) 5364–5457.
[7] G. Wang, L. Zhang, J. Zhang, A review of electrode materials for electrochemical supercapacitors, Chem. Soc. Rev. 41 (2012) 797–828.
[8] D.P. Dubal, O. Ayyad, V. Ruiz, P. Gómez-Romero, Hybrid energy storage: the merging of battery and supercapacitor chemistries, Chem. Soc. Rev. 44 (2015) 1777–1790.
[9] S. Zheng, X. Li, B. Yan, Q. Hu, Y. Xu, X. Xiao, H. Xue, H. Pang, Transition-metal (Fe, Co, Ni) based metal-organic frameworks for electrochemical energy storage, Adv. Energy Mater. 7 (2017) 1602733–1602760.
[10] S.K. Shinde, H.M. Yadav, G.S. Ghodake, A.A. Kadam, V.S. Kumbhar, J. Yang, K. Hwang, A.D. Jagadale, S. Kumar, D.Y. Kim, Using chemical bath deposition to create nanosheet-like CuO electrodes for supercapacitor applications, Colloids and Surfaces B. 181 (2019) 1004–1011.
[11] A.K. Mishra, A.K. Nayak, A.K. Das, D. Pradhan, Microwave-assisted solvothermal synthesis of cupric oxide nanostructures for high-performance supercapacitor, J. Phys. Chem. C 122 (2018) 11249–11261.
[12] D.P. Dubal, N.R. Chodankar, D. Kim, P.G. Romero, Towards flexible solid-state supercapacitors for smart and wearable electronics, Chem. Soc. Rev. 47 (2018) 2065–2129.
[13] X. Zhang, W. Shi, J. Zhu, D.J. Kharistal, W. Zhao, B.S. Lalia, H.H. Hng, Q. Yan, High-power and high-energy-density flexible pseudocapacitor electrodes made from porous CuO nanobelts and single-walled carbon nanotubes, ACS Nano 5 (2011) 2013–2019.
[14] R. Wu, D.P. Wang, V. Kumar, K. Zhou, A.W.K. Law, P.S. Lee, J. Lou, Z. Chen, MOFs-derived copper sulfides embedded within porous carbon octahedra for electrochemical capacitor applications, Chem. Commun. 51 (2015) 3109–3112.
[15] K. Wang, X. Dong, C. Zhao, X. Qian, Y. Xu, Facile synthesis of Cu_2O/CuO/RGO nanocomposite and its superior cyclability in supercapacitor, Electrochim. Acta 152 (2015) 433–442.
[16] D.P. Dubal, G.S. Gund, R. Holze, H.S. Jadhav, C.D. Lokhande, C. Park, Surfactant-assisted morphological tuning of hierarchical CuO thin films for electrochemical supercapacitors, Dalton Trans. 42 (2013) 6459–6467.
[17] Y. Liu, X. Cao, D. Jiang, D. Jia, J. Liu, Hierarchical CuO nanorod arrays in situ generated on three-dimensional copper foam via cyclic voltammetry oxidation for high-performance supercapacitors, J. Mater. Chem. A 6 (2018) 10474–10483.
[18] P. Xu, J. Liu, T. Liu, K. Ye, K. Cheng, J. Yin, D. Cao, G. Wang, Q. Li, Preparation of binder-free CuO/Cu_2O/Cu composites: a novel electrode material for supercapacitor applications, RSC Adv. 6 (2016) 28270–28278.
[19] L. Chen, Y. Zhang, P. Zhu, F. Zhou, W. Zeng, D.D. Lu, R. Sun, C. Wong, Copper salts mediated morphological transformation of Cu_2O from cubes to hierarchical flower-like or microspheres and their supercapacitors performances, Sci. Rep. 5 (2015) 9672–9679.
[20] J. Zhang, G. Zhang, W. Luo, Y. Sun, C. Jin, W. Zheng, Graphitic carbon coated CuO hollow nanospheres with penetrated mesochannels for high-performance asymmetric supercapacitors, ACS Sustain. Chem. Eng. 5 (2017) 105–111.
[21] Y. Liu, H. Huang, X. Peng, Highly enhanced capacitance of CuO nanosheets by formation of CuO/SWCNT networks through electrostatic interaction, Electrochim. Acta 104 (2013) 289–294.
[22] D.P. Dubal, G.S. Gund, R. Holze, C.D. Lokhande, Mild chemical strategy to grow micro-roses and micro-woolen like arranged CuO nanosheets for high performance supercapacitors, J. Power Sources 242 (2013) 687–698.
[23] J.S. Sagu, T.A.N. Peiris, K.G.U. Wijayantha, Rapid and simple potentiostatic deposition of copper (II) oxide thin films, Electrochem. Commun. 42 (2014) 68–71.
[24] X. Shu, Y. Wang, J. Cui, G. Xu, J. Zhang, W. Yang, M. Xiaoa, H. Zheng, Y. Qin, Y. Zhang, Z. Chen, Y. Wu, Supercapacitive performance of single phase CuO nanosheet arrays with ultra-long cycling stability, J. Alloys Compd. 753 (2018) 731–739.
[25] S.K. Shinde, D.-Y. Kima, G.S. Ghodake, N.C. Maile, A.A. Kadam, D.S. Lee, M.C. Rath, V.J. Fulari, Morphological enhancement to CuO nanostructures by electron beam irradiation for biocompatibility and electrochemical performance, Ultrason. Sonochem. 40 ((2018) 314–322.
[26] K. Chen, D. Xue, Room-temperature chemical transformation route to CuO nanowires toward high-performance electrode materials, J. Phys. Chem. C 117 (2013) 22576–22583.
[27] L. Wang, W. Cheng, H. Gong, C. Wang, D. Wang, K. Tang, Y. Qian, Facile synthesis of nanocrystalline-assembled bundle-like CuO nanostructure with high rate capacities and enhanced cycling stability as an anode material for lithium-ion batteries, J. Mater. Chem. 22 (2012) 11297–11302.
[28] S.K. Shinde, D.P. Dubal, G.S. Ghodake, D.Y. Kim, V.J. Fulari, Nanoflower-like CuO/Cu$(OH)_2$ hybrid thin films: synthesis and electrochemical supercapacitive properties, J. Electroanal. Chem. 732 (2014) 80–85.
[29] A.C. Nwanya, D. Obi, K.I. Ozoemena, R.U. Osuji, C. Awada, A.R.M. Maaza, F. Rosei, F.I. Ezema, Facile synthesis of nanosheet-like CuO film and its potential application as a high-performance pseudocapacitor electrode, Electrochim. Acta 198 (2016) 220–230.
[30] K. Padrón, E.J. Juárez-Pérez, F. Forcade, R. Snyders, X. Noirfalise, C. Laza, J. Jiménez, E. Vigil, Nanostructured CuO films deposited on fluorine doped tin oxide conducting glass with a facile technology, Thin Solid Films 660 (2018) 386–390.
[31] A. Lamberti, M. Fontana, S. Bianco, E. Tresso, Flexible solid-state Cu_xO-based pseudo-supercapacitor by thermal oxidation of copper foils, Int. J. Hydrog. Energy 41 (2016) 11700–11708.
[32] J. Zhao, X. Shu, Y. Wang, C. Yu, J. Zhang, J. Cui, Y. Qin, H. Zheng, J. Liu, Y. Zhang, Y. Wu, Construction of CuO/Cu_2O@CoO core shell nanowire arrays for high-performance supercapacitors, Surf. Coat. Technol. 15 (2016) 15–21.
[33] I.Y.Y. Bu, R. Huang, Fabrication of CuO-decorated reduced graphene oxide nanosheets for supercapacitor applications, Ceram. Int. 43 ((2017) 45–50.
[34] H. Chen, J. Chen, Preparation of p-type $CuCo_2O_4$ thin films by sol-gel processing, Mater. Lett. 188 (2017) 63–65.
[35] D. He, G. Wang, G. Liu, J. Bai, H. Suo, C. Zhao, Facile route to achieve mesoporous Cu$(OH)_2$ nanorods on copper foam for high-performance supercapacitor electrode, J. Alloys Compd. 699 (2017) 706–712.

[36] P. Venkateswari, P. Thirunavukkarasu, M. Ramamurthy, M. Balaji, J. Chandrasekaran, Optimization and characterization of CuO thin films for P–N junction diode application by JNSP technique, Optik 140 (2017) 476–484.
[37] C. Wan, Y.J. Jian Li, Multilayer core–shell structured composite paper electrode consisting of copper, cuprous oxide and graphite assembled on cellulose fibers for asymmetric supercapacitors, J. Power Sources 361 (2017) 122–132.
[38] F. Gao, L. Zhu, H. Li, H. Xie, Hierarchical flower-like CuO film: one-step room temperature synthesis, formation mechanism and excellent optoelectronic properties, Mater. Res. Bull. 93 (2017) 342–351.
[39] M. Ponnar, C. Thangamani, P. Monisha, S.S. Gomathi, K. Pushpanathan, Influence of Ce doping on CuO nanoparticles synthesized by microwave irradiation method, Appl. Surf. Sci. 449 (2018) 132–143.
[40] A. Gopalakrishnan, N. Vishnu, S. Badhulika, Cuprous oxide nanocubes decorated reduced graphene oxide nanosheets embedded in chitosan matrix: a versatile electrode material for stable supercapacitor and sensing applications, J. Electroanal. Chem. 834 (2019) 187–195.
[41] H.R. Barai, M. Rahman, M. Roy, P. Barai, S. WooJoo, A calcium doped binary strontium-copper oxide electrode material for high-performance supercapacitors, Mater. Sci. Semicond. Process. 90 (2019) 245–251.
[42] S.V. Mohite, V.V. Ganbavle, K.Y. Rajpure, Solar photoelectrocatalytic activities of rhodamine-B using sprayed WO_3 photoelectrode, J. Alloys Compd. 655 (2016) 106–113.
[43] D.-Y. Kim, G.S. Ghodake, N.C. Maile, A.A. Kadam, D. Sung Lee, V.J. Fulari, S.K. Shinde, Chemical synthesis of hierarchical $NiCo_2S_4$ nanosheets like nanostructure on flexible foil for a high performance supercapacitor, Sci. Rep. 7 (2017) 9764–9773.
[44] S.K. Shinde, M.B. Jalak, G.S. Ghodake, N.C. Maile, V.S. Kumbhar, D.S. Lee, V.J. Fulari, D.-Y. Kim, Chemically synthesized nanoflakes-like $NiCo_2S_4$ electrodes for high-performance supercapacitor application, Appl. Surf. Sci. 466 (2019) 822–829.
[45] V. Senthilkumar, Y.S. Kim, S. Chandrasekaran, B. Rajagopalan, E.J. Kim, J.S. Chung, Comparative supercapacitance performance of CuO nanostructures for energy storage device applications, RSC Adv. 5 (2015) 20545–20553.
[46] J. Fan, D. Tang, D. Wang, Spontaneous growth of CuO nanoflakes and microflowers on copper in alkaline solutions, J. Alloys Compd. 704 (2017) 624–630.
[47] C. Huang, W. Ye, Q. Liu, X. Qiu, Dispersed Cu_2O octahedrons on h-BN nanosheets for p-nitrophenol reduction, ACS Appl. Mater. Interfaces 6 (2014) 14469–14476.
[48] S.K. Shinde, V.J. Fulari, D.-Y. Kim, N.C. Maile, R.R. Koli, H.D. Dhaygude, G.S. Ghodake, Chemical synthesis of flower-like hybrid $Cu(OH)_2$/CuO electrode: application of polyvinyl alcohol and triton X-100 to enhance supercapacitor performance, Colloid Surface B 156 (2017) 165–174.
[49] S.K. Shinde, G.S. Ghodake, V.J. Fulari, D.-Y. Kim, High electrochemical performance of nanoflakes like CuO electrode by successive ionic layer adsorption and reaction (SILAR) method, J. Ind. Eng. Chem. 52 (2017) 12–17.
[50] S.K. Shinde, J.V. Thombare, D.P. Dubal, V.J. Fulari, Electrochemical synthesis of photosensitive nano-nest like $CdSe_{0.6}Te_{0.4}$ thin films, Appl. Surf. Sci. 282 (2013) 561–565.
[51] S.E. Moosavifard, M.F. El-Kady, M.S. Rahmanifar, R.B. Kaner, M.F. Mousavi, Designing 3D highly ordered nanoporous CuO electrodes for high performance asymmetric supercapacitors, ACS Appl. Mater. Interfaces 7 (2015) 4851–4860.
[52] Y.X. Zhang, M. Huang, M. Kuang, C.P. Liu, J.L. Tan, M. Dong, Y. Yuan, X.L. Zhao, Z. Wen, Facile synthesis of mesoporous CuO nanoribbons for electrochemical capacitors applications, Int. J. Electrochem. Sci. 8 (2013) 1366–1381.
[53] G. Wang, J. Huang, S. Chen, Y. Gao, D. Cao, Preparation and supercapacitance of CuO nanosheet arrays grown on nickel foam, J. Power Sources 196 (2011) 5756–5760.
[54] S. Nakayama, A. Kimura, M. Shibata, S. Kuwabata, T. Osakai, Voltammetric characterization of oxide films formed on copper in air, J. Electrochem. Soc. 148 (2001) 467–472.
[55] M. Kang, A.A. Gewirth, Voltammetric and force spectroscopic, examination of oxide formation on Cu(111) in basic solution, J. Phys. Chem. B 106 (2002) 12211–12220.
[56] S.K. Shinde, D.P. Dubal, G.S. Ghodake, V.J. Fulari, Hierarchical 3D-flower-like CuO nanostructure on copper foil for supercapacitors, RSC Adv. 5 (2015) 4443–4447.
[57] S.K. Shinde, D.P. Dubal, G.S. Ghodake, P.G.- Romero, S. Kim, V.J. Fulari, Influence of Mn incorporation on the supercapacitive properties of hybrid CuO/$Cu(OH)_2$ electrodes, RSC Adv. 5 (2015) 30478–30484.
[58] M.B. Gholivand, H. Heydari, A. Abdolmaleki, H. Hosseini, Nanostructured CuO/PANI composite as supercapacitor electrode material, Mater. Sci. Semicond. Process. 30 (2015) 157–161.
[59] D.P. Dubal, G.S. Gund, C.D. Lokhande, R. Holze, CuO cauliflowers for supercapacitor application: novel potentiodynamic deposition, Mater. Res. Bull. 48 (2013) 923–928.
[60] A. Pendashteh, S.E. Moosavifard, M.S. Rahmanifar, Y. Wang, M.F. El-Kady, R.B. Kaner, M.F. Mousavi, Highly ordered mesoporous $CuCo_2O_4$ nanowires, a promising solution for high-performance supercapacitors, Chem. Mater. 27 (2015) 3919–3926.
[61] P.C. Rath, J. Patra, D. Saikia, M. Mishra, C.M. Tseng, J. Chang, H. Kao, Comparative study on the morphology-dependent performance of various CuO nanostructures as anode materials for sodium-ion batteries, ACS Sustain. Chem. Eng. 6 (2018) 10876–10885.
[62] M. Harilal, B. Vidyadharan, I.I. Misnon, G.M. Anilkumar, A. Lowe, J. Ismail, M.M. Yusoff, R. Jose, One-dimensional assembly of conductive and capacitive metal oxide electrodes for high-performance asymmetric supercapacitors, ACS Appl. Mater. Interfaces 9 (2017) 10730–10742.
[63] F. Daneshvar, A. Aziz, A.M. Abdelkader, T. Zhang, H. Sue, M.E. Welland, Porous SnO_2–Cu_xO nanocomposite thin film on carbon nanotubes as electrodes for high performance supercapacitors, Nanotechnology 30 (2019) 015401–015410.